

Electric field distribution in 132 kV XLPE cable termination model from finite element method

H. A. Illias, Q. L. Ng, A. H. A. Bakar, H. Mokhlis
UMPEDAC
Electrical Engineering Department
Faculty of Engineering, University of Malaya
Kuala Lumpur, Malaysia
h.illias@um.edu.my

A. M. Ariffin
College of Engineering
Universiti Tenaga Nasional
Selangor, Malaysia

Abstract—High voltage cable terminations are widely used in power system networks. A proper design of cable termination is essential in reducing the electric field distribution around the end of high voltage cable. However, if there are defects exist at cable termination structure, the electric field can be enhanced significantly and can be the source of electrical discharges. Therefore, it is important to understand the effect of defects on the electric field distribution at cable terminations. In this work, a 132 kV XLPE outdoor cable termination has been modelled using finite element analysis (FEA) method. The model has been used to simulate the electric field distribution in the cable termination in the presence of defects. Defects that have been considered are void defect in porcelain, stress cone and fluid, sharp pin on the porcelain surface and delamination defect between the insulator and the stress cone. The effect of different void location, material dielectric constant and porcelain radius on the electric field magnitude at cable termination have also been investigated. From the results obtained in this work, a better understanding of the electric field distribution at the cable termination with defects can be attained.

Keywords- cable termination, electric field, finite element analysis

I. INTRODUCTION

High voltage power cable terminations are of great importance in transmission and distribution of power system. The termination of a cable acts as a shield in the outer phase of the end of a cable to prevent the leakage of the electric field [1]. The leakage of the electric field is the source of partial discharge phenomenon, which may cause failure of the cable insulation. Partial discharges normally occur at the defect side within the insulation layer. Defects exist during the process of cable moulding, where air may be trapped inside the cable insulation and can be the potential source of partial discharges. Therefore, study the electric field distribution in the structure of cable terminations is important.

Nowadays, there are many types of cable termination, such as oil-filled cable outdoor termination, XLPE cable outdoor termination, and XLPE cable SF₆ termination. These cable terminations are used based on their applications [2, 3]. For oil-filled cable outdoor termination, they are normally used at undersea cable transition due to the characteristic of oil that resists to water. For wipe air moisture, SF₆ termination is preferable because SF₆ has a high dielectric strength, non-flammable and chemically non-reactive. XLPE cable

termination is normally used in transmission and distribution systems because XLPE has strong bond properties in its molecular structure.

Power cables are very important in transmission and distribution systems. There are two main components of power cables, they are terminations and joints. At cable termination, power cables are shielded by an electrical stress control in cable installation. Without the insulation shield, high potential gradients are concentrated at the cutback point, causing high electrical stress. Electric field enhancement at these points can cause the occurrence of electrical discharges. This could lead to flashover along the insulation surface or dielectric breakdown, causing cable failure [4-6]. Therefore, a proper design of cable termination is important to eliminate the stress concentration at the termination to avoid the breakdown of the cable.

In this work, a model geometry of a 132 kV XLPE cable outdoor termination has been modeled using finite element analysis (FEA) software. The model has been used to obtain the electric field distribution in the model with various types of defects at cable termination through simulation. The effects of different material properties and dimension of the cable termination geometry on the electric field distribution have been investigated. The information obtained from the simulation results may be able to help in cable termination design to reduce the electric field magnitude.

II. FEA MODEL

Figure 1 shows a two-dimensional (2D) axial symmetric model geometry of a 132 kV XLPE cable outdoor termination that has been developed using FEA software. Table 1 shows the dielectric constant of each component in the model that has been developed. The conductor is applied with a 132 kV voltage amplitude, the conductor stalk is assigned as a floating potential and all internal boundaries are continuity.

III. SIMULATION RESULTS

A. Electric field distributions using FEA method

Figure 2 shows the electric field distribution of 132 kV XLPE outdoor termination without any defects from the simulation model. The colour map in Figure 2 represents the electric field magnitude. The electric field can be seen concentrated at the edge of conductor stalk while other regions in the cable termination have a lower electric field magnitude.

This project was sponsored by University of Malaya, Malaysia

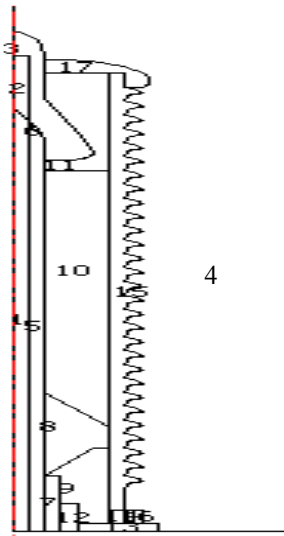


Figure 1. 2D axial-symmetric 132 kV XLPE cable termination model

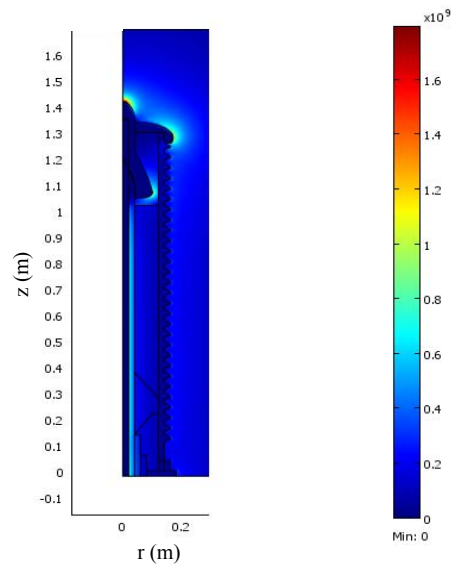
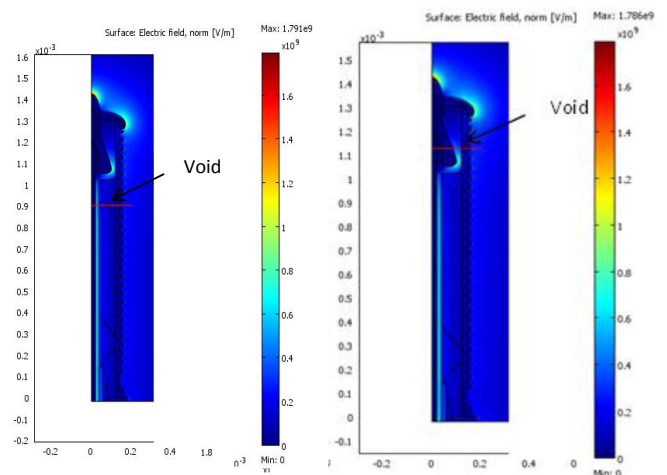


Figure 2. Simulated electric field distribution

TABLE I. DIELECTRIC CONSTANT OF COMPONENTS IN 132 kV XLPE CABLE TERMINATION MODEL

Component	Dielectric constant
Conductor (1)	1
Conductor stalk (2, 3, 6)	1
Air (4, 11)	1
XLPE (5)	2.5
Parafin (7)	2.5
Stress cone (8)	3.6
Silicon resin, liquid (9, 10)	3.5
Alumina, silicone dioxide (12)	4.5
Porcelain (13-16)	6
Cover of conductor stalk (17)	1

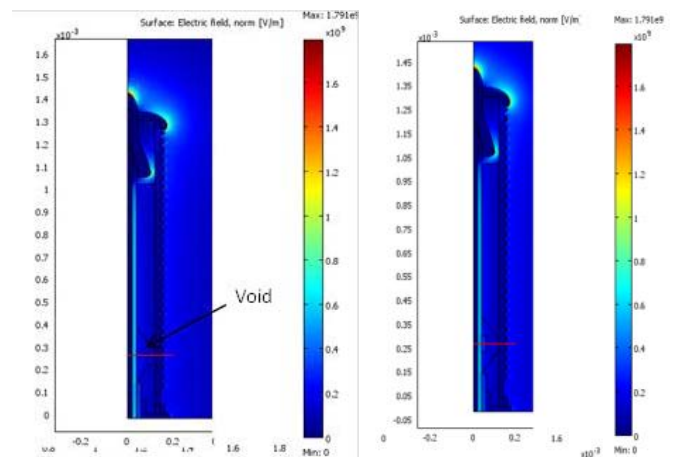


(a) Void inside the silicone fluid

(b) Void inside the porcelain

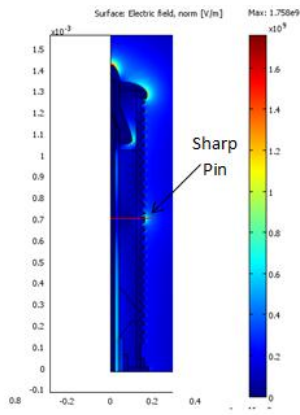
Figure 3 shows the model geometry with different types of defect; they are a void within the silicone fluid, porcelain and stress cone, a sharp pin on the porcelain surface and a delamination defect. When there is a void defect, a lower dielectric constant of the void than the surrounding insulation material causes the electric field in the void to be higher than the surrounding material. This can be seen clearly from the cross section of electric field magnitude across the void region when compared to the model without void defect in Figures 4a to 4c. Partial discharge may occur within the void when the electric field in the void is higher than the breakdown strength of the gas. A delamination defect also causes the electric field to be enhanced as similar to void defects in insulation material, as shown in Figure 4d. However, surface discharges can occur within the delamination air gap due to its elongated geometry. During the process of lamination, an air gap or delamination appears due to air trapped within the lamination layer.

Figure 3e shows a model geometry of cable termination where a sharp pin exists on the insulation surface. There is a



(c) Void in the stress cone

(d) Air gap between stress cone and cable



(e) Sharp pin embedded into porcelain

Figure 3. Simulated electric field distribution with various defects

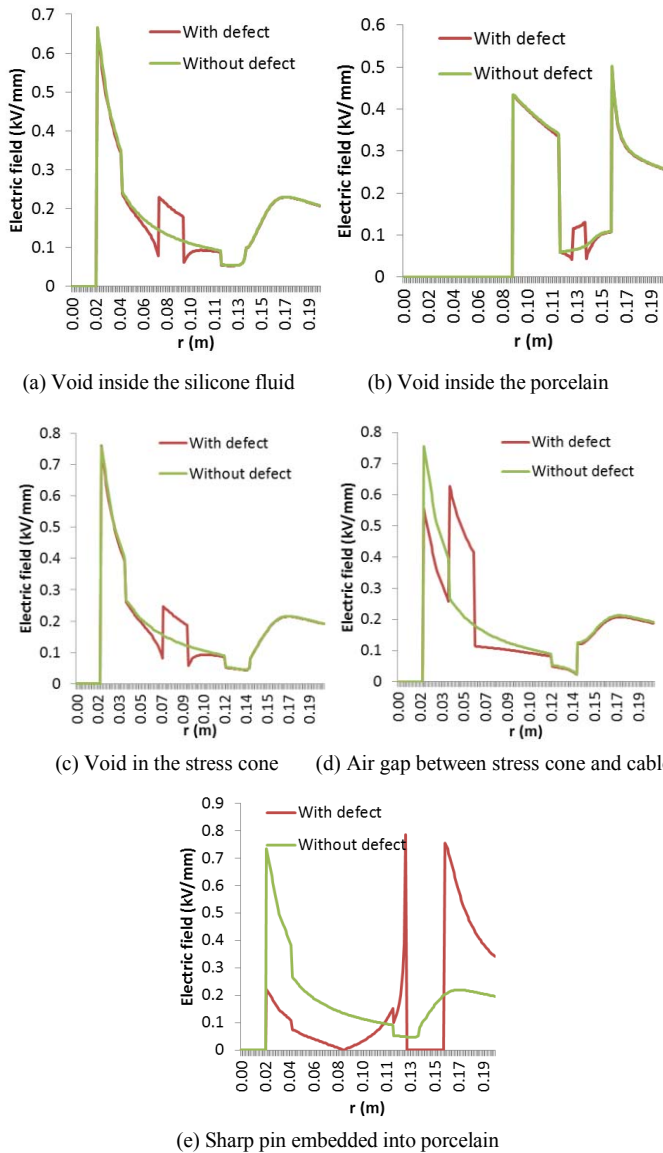


Figure 4. Cross section plot of the electric field magnitude in the cable joint models with and without defects along $z = 0$ line

potential of corona discharge to occur because the electric field at the sharp pin is enhanced drastically, as can be seen clearly from the cross section of electric field magnitude across the void region when compared to the model without void defect (Figure 4e). When corona discharge occurs, it causes progressive electric discharge to occur from the sharp pin, causing power loss.

B. Effect of dielectric constant on the electric field

The cross section plot of the electric field magnitude across a spherical void within the porcelain bushing of different dielectric constant, ϵ_r from the FEA model geometry is shown in Figure 5. The centre of the void is located at $r = 0.18$ m and $z = 1$ m, as shown in Figure 6. The red line in Figure 6 shows the electric field magnitude that is plotted in Figure 5. It can be seen that the electric field magnitude in the void becomes lower when the dielectric constant of the bushing increases. This can be seen clearly in Figure 7, where the maximum electric field in the void decreases with the bushing dielectric constant. When the bushing dielectric constant increases, the alignment of the electric field in the bushing is better. This results in less electric field concentration in the material and around the void. Therefore, the electric field in the void also decreases.

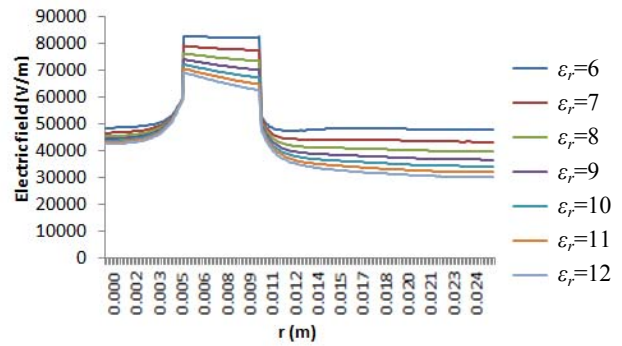


Figure 5. Cross-section plot of electric field magnitude within the void with different dielectric constant of porcelain bushing in XLPE cable termination

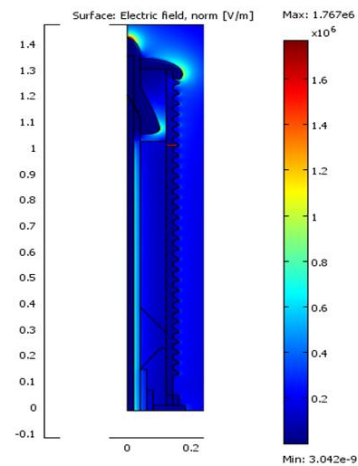


Figure 6. Void at $r = 0.18$ m and $z = 1$ m within XLPE cable termination

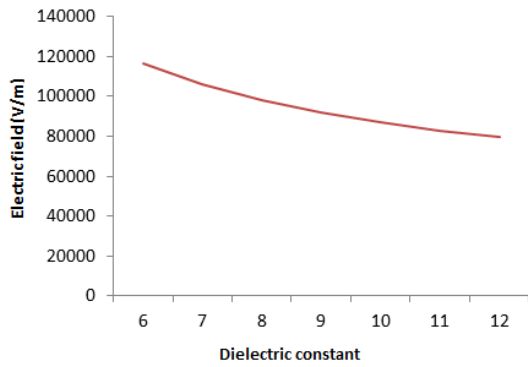


Figure 7. Electric field magnitude in the centre of the void as a function of dielectric constant of porcelain from Figure 6

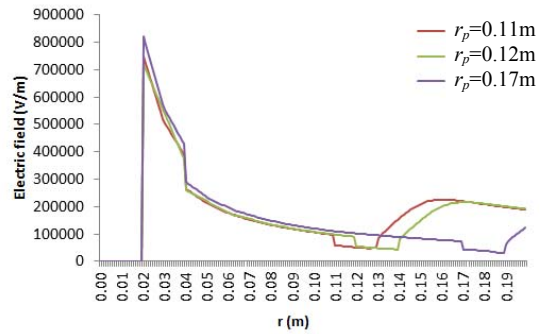


Figure 9. Cross section plot of electric field magnitude using different radius of porcelain in XLPE cable outdoor termination

C. Effect of void locations on the electric field magnitude

Figure 8 shows the electric field magnitude in the centre of a void located within the porcelain bushing when the void location is varied along the z-axis ($z = 0.3$ to $z = 2.1$ m) at $r = 0.2$ m. The electric field is almost constant from $z = 0.3$ m until 0.7 m before increases from $z = 0.7$ m. The void that is located nearer to the aluminium cap has higher electric field due to the high electric field at the aluminium cap. Thus, the electric field in the void is influenced by the location of the void.

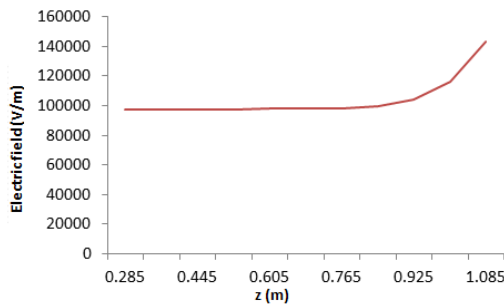


Figure 8. Electric field magnitude in the void at different location in the porcelain of XLPE cable termination model geometry

D. Effects of porcelain radius on the electric field magnitude

Figure 9 shows the cross sectional plots of the electric field magnitude along $z = 0.25$ m line in the model geometry shown in Figure 1 with different radius, r_p of the porcelain bushing. It is used to study the effect of the bushing radius on the electric field distribution in the model. Referring to Figure 9, a larger radius of the porcelain bushing causes lower electric field at the interface of air-stress cone but the region of higher electric field in air is wider. For a smaller radius of the porcelain bushing, the electric field at the interface of air-stress cone is higher but the region of higher electric field in air is less. Therefore, a suitable radius of the porcelain bushing is important in controlling the electric field distribution and the cost of the materials in cable termination structures.

IV. CONCLUSIONS

A model geometry of 132 kV cable terminations has been successfully developed using finite element analysis (FEA) software to simulate the electric field distributions in the cable termination. Comparison between the model with and without defects shows that when there are defects exist in a cable termination, the electric field is distorted across the defect. The electric field is enhanced significantly at the defect region due to a lower dielectric constant than the surrounding material. These defects can be the source of partial discharge phenomena, which can affect the performance of the cable termination. It was also found that the dielectric constant of the insulation material, porcelain radius and location of the void within the bushing influence the electric field distribution and magnitude in the cable termination. Therefore, this information may assist in designing a model of cable termination to improve the electric field distribution.

ACKNOWLEDGMENT

The author thanks the University of Malaya for supporting this work through the HIR research grant (Grant no: H-16001-00-D000048).

REFERENCES

- [1] G. Bas, "Electric field analysis in stress controlled high voltage cables," M.Sc. Thesis, Middle East Technical University, Turkey, 2005.
- [2] W. A. Thue, "Electrical Power Cable Engineering," 2nd ed, Marcel Dekker, 2003.
- [3] L. Heinhold, "Power Cables and Their Application," 3rd ed, Siemens Aktiengesellschaft, 1993.
- [4] J. H. Mason, "The deterioration and breakdown of dielectrics resulting from internal discharges," IEE proceedings, 98, 1951, pp. 44-59.
- [5] H. Illias, G. Chen and P. L. Lewin, "Modelling of partial discharge activity in spherical cavities within a dielectric material," IEEE Electrical Insulation Magazine, 27, 2011, pp. 38-45.
- [6] H. Illias, G. Chen and P. L. Lewin, "The influence of spherical cavity surface charge distribution on the sequence of partial discharge events," J. Phys. D: Appl Phys., 44, 2011, pp. 1-15.